Indian Journal of Biochemistry & Biophysics
Vol. 62, November 2025, pp. 1258-1276
DOI: 10.56042/ijbb.v62i11.18341

Bioinformatic analysis of cervical cancer-associated hub genes and repurposing of 5-fluorouracil and gemcitabine as potential therapeutic agents

Deepika Shekhawat[1], Vaddi Damodara Reddy[1], Gouthami Kuruvalli[2,3]*, Althaf Hussain Shaik[4]* & Hymavathi Reddyvari[5]

[1]Department of Biotechnology School of Applied Sciences, Reva University, Bangalore -560 064, Karnataka, India

[2]Department of Biochemistry School of Allied Health Sciences, Reva University, Bangalore -560 064, Karnataka, India

[3]Department of Zoology, College of Science, King Saud University, Riyadh-11451, Saudi Arabia

[4]DR Biosciences, Research and Development Unit, Ganganagar, Bettahalasur, Bangalore-56215, Karnataka, India

[5]Section of Thoracic surgery, Lewis Katz School of Medicine, Temple University, Philadelphia, PA 19122, USA

Received 28 March 2025; *revised 17 June 2025*

Cervical cancer represents a major health issue worldwide. This study aimed to identify hub genes and signaling pathways associated with cervical cancer, and evaluate the efficacy of FDA-approved drugs against these hub proteins. From the Gene Expression Omnibus (GEO), we identified 239 genes (GSE26511) and 248 genes (GSE41827) that are differentially expressed in cervical cancer, which include 145 genes that are up-regulated and 94 that are down-regulated, along with 174 up-regulated genes and 74 down-regulated genes. By protein-protein interaction network (PPI) indicated 6 key genes for GSE26511 (ID2, FGF2, CLIC4, MED14, NGEF, TCF4) and 6 key genes for GSE41827 (ATF3, BCL2, MAF, MYC, TP53, HMOX). Molecular docking analysis of FDA-approved drugs (5-fluorouracil and gemcitabine) against 12 key proteins revealed potent binding affinities, with ID2 shown binding affinity of -5.2 kcal/mol when interacting with 5-fluorouracil, while CLIC4 shown a binding affinity of -7.2 kcal/mol with gemcitabine, along with 5 hydrogen bonds. Furthermore, MYC exhibit strong binding affinity with both drugs, and TP53 displayed a binding affinity of -5.6 kcal/mol with 5-fluorouracil and gemcitabine with hydrogen bonds. These results indicate that key proteins identified from the study show enhanced binding affinities with FDA-approved drugs, offering insights for targeted therapies in cervical cancer.

Keywords: ADMET, Cervical cancer, Cytoscape, Differentially expressed genes, Gene expression omnibus

Despite the fact that Cervical cancer is preventable, but according to the estimation of the reports, it is considered as the fourth most common cancer caused in women across the globe, with the approximate number of 570, 000 women suffering from it and 311, 000 related deaths in 2018. Although the rate of cervical cancer has reduced in the developed country such as United states but is the concern for the death related to cervical cancer in the countries which are at the phase of developing. Many recommendations on the treatment of cervical cancer are established, which includes their screening and diagnosis. According to the recent recommendation based on the combination of advanced therapies, which includes immuneotherapy and targeted therapy, when combined with traditional first- and second-line treatments, has led to improved outcomes in the cervical cancer patients[1]. Despite the accessibility of vaccines and method available in advanced screening, it was projected by the Cancer Stat Facts that cervical cancer will take the lives of approximately 4, 280 lives in the United States in the year 2022. Globally, 604, 000 new cases and 342, 000 deaths in 2020 was reported by the World Health Organization (WHO), and majority of cases were found in the countries with lower- and middle-class income countries[2].The predominately agent of cervical cancer, which causes this chronic disease is the high-risk papillomavirus (HR-HPV) genotypes. Although numerous intervention methods and screening tests are available but still when the cases are detected at the later stage are hard to be treated. At present, the palliative platinum-based chemotherapy (CT) available for the first-line treatment of recurrent cervical or metastatic is considered to be the standard, but the chances of survival and recovery are not in the favorable situation. But on the other hand, the targeted therapy has demonstrated the effective outcomes in the survival rated of the patients. Our understanding advancements in the cervical cancer genome and

*Correspondence:
E-mail: gouthamiv2023@yahoo.com (GK); salthaf@ksu.edu.sa (AHS)
Suppl. data available on respective page of NOPR

further identifying the targets for the therapy will hold a potential for the advanced and new treatments for the cervical cancer[3]. The process called metastasis is where the cervical cancer aggressively spread to the area nearby it and also to the organs in close proximity. The cells can spread to the lymphatic system and often spread to the pelvic lymph nodes. During this whole process, the cancer cells get the adaptation and survival by activation of certain genes and pathways for their fitness, and instead, the immune system fighting against the tumor cells helps them to spread and grow further. Despite having the understanding, it is still unclear about the molecular mechanism and invasion of cervical cancer and spreading inside the lymph nodes[4]. In the process of post transcriptional mechanism of the gene expression regulation, microRNAs are involved, which are also known as to be the key components of the non-coding RNA family approximately 18-25 nucleotides in size are involved in expression in various kinds of malignancies, which either functions as tumor suppressors or oncogenes[5].The two key proteins which are known as E6 and E7, present in the high-risk human papillomavirus (HPV) main cause of CC, are expressed in tumor cells and are considered to be the ideal targets as they are involved in Tumorigenesis and maintains the cancerous characteristics[6]. The transcriptome data analysis is a needful tool to analyse the genes expression data and find out the hub genes which plays the critical roles in the diseases. Gene Expression Omnibus (GEO) and GREIN are the public database available online, and so far, many studies have been conducted and published using them to foresee the potential biomarkers involved in the diseases[7]. According to a study conducted, it was seen that the expression of the genes KLF4 and ESR1 was down-regulated by the miR21 and miRNA16 up-regulation in the cervical cancer, and this down-regulation is related to poor prognosis, which means severity in the diseases this connection suggests that the lower expression of the genes KLF4 and ESR1 might serve as biomarkers and help in the prediction and diagnosis of the CC at early stage[8].

Materials and Methods

Identification and Examination of Differentially Expressed Genes (DEG's)

The Gene Expression Omnibus database from NCBI was used to collect the data from the Cervical cancer patient (http://www.ncbi.nlm.nih.gov/geo)[9]. The data was collected by using the GSE26511 and GSE41827 datasets that contains the expression profile of the cervical cancer. The GSE26511 included the expression profile of 5 positive sample of Cervical cancer lymph node patient with accession number GSM651851, GSM651852, GSM651853, GSM651854, GSM651855 and 5 control samples with accession number GSM651831, GSM651832, GSM651833, GSM651834, GSM651835. The GSE41827 datasets includes analysis of cervical cancer HeLa cells treated with casiopeinas II-gly (40 μM) for 6 hours with 3 control and 3 positive samples. The cervical cancer (Hela) cell line with 3 controls has accession number GSM1025049, GSM1025050, GSM1025051 and the 3 positive Hela cells treated with cas II- gly with accession number GSM1025052, GSM1025053, GSM1025054. The raw gene expression data taken from NCBI was analysed using the tool GEO2 (https://www.ncbi.nlm.nih.gov/geo/geo2r/?acc=GSE26511 and GSE41827) for differential GEO data expression[10]. We established the primary criteria for identifying significant differentially expressed genes (DEGs) as | log (fold change) | > 1 and $P< 0.05$. Up-regulated DEGs were considered with a log FC > 1, while down-regulated DEGs had a log FC < -1[11]. The up-regulated and down-regulated genes were divided of both GSE26511 and GSE41827. The GSE26511 has 239 genes out of which 145 are up-regulated and 94 are down-regulated and 50 were selected from each. The GSE41827 also has 248 genes 174 up-regulated and 74 down-regulated and 50 were taken accordingly from both for making heatmap and further studies.

DEGs Functional and pathway Enrichment Analysis

The functional gene enrichment analysis was performed by FUNRICH (Functional enrichment analysis tools)[12] and DAVID enrichment analysis[13], for biological pathway analysis and functions associated with the genes[14]. Different options available were utilized for the enrichment analysis, such as cellular component, biological process, molecular function. The results of these analyses were then visually represented in a column chart[15].

PPI network and Hub genes analysis

To find the correlation of DEGs they were mapped to an online database tool STRING (https://string-db.org/) for the protein-protein interaction (PPI) and

visualized in cystoscope[16]. The MCODE (Molecular Complex Detection) application was employed to detect genes with notable interactions within the PPI network, arranging them into modules. This was accomplished by setting a degree cutoff parameter of ≥3, while keeping the default settings for other parameters: a Node Score cutoff of ≥2, a K-Core of ≥2, and a Maximum Depth of 100[17]. The CytoHubba plugin in Cytoscape was employed to pinpoint the hub genes within the PPI network. This was done using the MCC rank method, which evaluates the degree of each protein node[18].

Protein prediction and active site analysis

The PPI analysis results provided the hub genes for further docking studies which were taken from RCSB Protein Data Bank (https://www.rcsb.org/). The FASTA sequence was taken from NCBI (https://www.ncbi.nlm.nih.gov/protein/)for each of the protein and selected the specific chain and used Blastp(https://blast.ncbi.nlm.nih.gov/Blast.cgi?PAGE=Proteins)[19,20] for Swiss modelling (https://swissmodel.expasy.org/)[21] and the best model was downloaded in PDB format once the stereochemical quality of the model was ensured using Ramachandran plot[22]. The active sites of each protein were subsequently evaluated using the CASTp[23] server and the protein as well as ligands were converted to PDBQT for further docking studies using AutoDock. The molecular docking studies was done on the 12 identified targets for the cervical cancer and the targets were identified using the PPI network. 6 targets were taken from GSE26511and other 6 from GSE41827. The GSE26511 has ID2, crystal structure of thymidine kinase from herpes simplex virus type i complexed with 5-iododeoxyuridine(PDB id: 1K17, resolution factor:2.20 Å), FGF2, Crystal structure of API5-FGF2 complex(PDB id: 6L4O resolution factor: 2.60 Å), CLIC4, Crystal structure of import in-alpha bound to a CLIC4 NLS peptide(PDB id: 3OQS, resolution factor: 2.00 Å), MED14, Tail module of Mediator complex (PDB id: 7JMN, resolution factor: 3.58 Å), NGEF, Crystal structure of DH-PH domain of RhoGEF3(Xpln) (PDB id: 2ZOQ, resolution factor: 1.79 Å), TCF4, Crystal Structure of a Human Tcf-4 / beta-Catenin Complex (PDB id:1JPW , resolution factor: 2.50 Å) as the targets whereas the GSE41827 has ATF3 Activating Transcription Factor 3 (UniProtKB/Swiss-Prot (P18847), BCL2, Crystal Structure of a Zebra-fish pro-survival protein NRZ:Bad BH3 complex (PDB id: 6FBX , resolution factor: 1.64 Å) MAF, crystal structure of bacillus subtilis maf protein(PDB id: 1EX2 , resolution factor: 1.85 Å). MYC The structure of the anti-c-myc antibody 9E10 Fab fragment (PDB id: 2ORB, resolution factor: 2.20Å) TP53 Co-crystal structure of 53BP1 tandem Tudor domains in complex with UNC9512(PDB id: 9CKJ, resolution factor: 2.25Å), HMOX Structure of heme oxygenase-2 containing residues 1-288 lacking the membrane spanning region (PDB id: 4WMH, resolution factor: 2.50Å) (Fig. 1).

Preparation of ligand

5-Flurouracil[24]andGemcitabine[25] are the FDA approved drugs. The PubChem database (https://pubchem.ncbi.nlm.nih.gov/) was used to retrieve the 3D structures of the drugs in SDF format[26] Biovia Discovery studio visualizer was used to convert into PDB format[27]. Next, MGL Tools 1.5.6 was used to add Gasteiger partial atomic charges (Q),

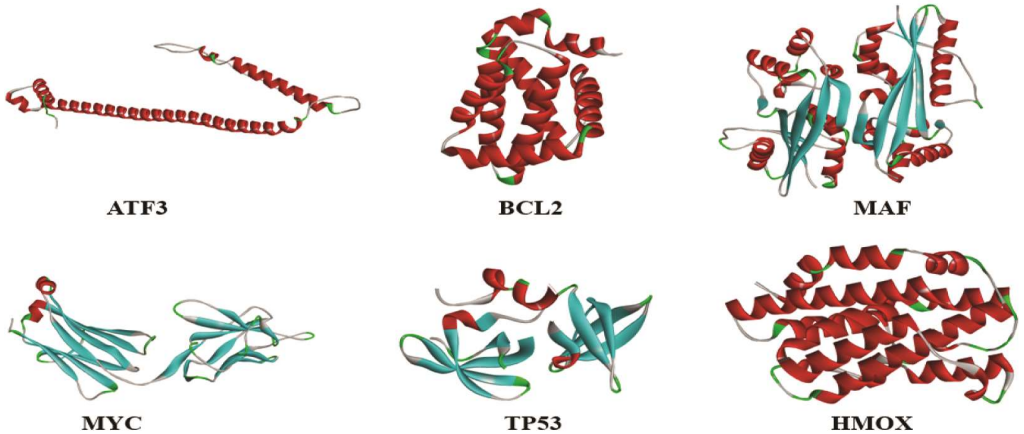

Fig. 1 — 3D structures of targeted genes from GSE26511 (ID2, FGF2, CLIC4, MED14, NGEF, TCF4) and GSE41827 (ATF3, BCL2, MAF, MYC, TP53, HMOX)

modify the atom type to Autodock4 (T) compatible mode, and save the data in PDBQT format[28].

Molecular descriptors (MDs)

The physiochemical properties of a chemical agent such as Molecular weight (MW), hydrogen bond donors (OHNH), topological polar surface area (TPSA), rotatable bonds (RB) and partition coefficient (log P) have an effect on it by its MD and the degree of penetration inside the cell depends upon the MDs increase in MDs value means decrease in the penetration inside the cell. Molinspiration (https://www.molinspiration.com/cgi/properties)[29] was used to calculate the MDs. The drug-like properties of specific ligands are predicted by the Lipinski rule of five. The rule of five states that an appropriate drug should have an octanol/water partition coefficient (QPlogPo/w) of less than or equal to five, a donor HB of less than or equal to five, and an acceptor HB of less than or equal to ten. A compound may be considered drug-like if it possesses all of these characteristics[30].

ADMET evaluation

Analysis of Pharmacokinetic Profile, Physicochemical properties and ADMET properties such as (absorption, distribution, metabolism, excretion, and toxicity) were determined by SwissADME (http://www.swissadme.ch/index.php). The Lipinski Rule of Five (RO5) is necessary for any Drug development if a single rule is violated the drug might have poor absorption or less permeability[31].

Brain or intestinal estimated (BOILED-Egg)

The SMILES were entered in the tool SwissADME (http://www.swissadme.ch/index.php)for generating the prediction model of the drug whether it has brain penetration (yes or no) and gastrointestinal absorption (high or low). The graphical representation is basically based on 2 parameters Wildman–Crippen method (WLogP) versus topological polar surface area (tPSA) value which is lipophilicity and polarity of the drug[32].

Results and Discussion

Identification of DEGs in breast cancer

After the microarray results have been standardized, we identified 239 DEGs in GSE26511 and 248 in GSE41827. Among these 239 DEGs of GSE26511, 145genes were up-regulated, and94 are down-regulated whereas for GSE41827, 174 were up-regulated and 74 down-regulated. Subsequently, the gene expression represents Control *vs* cervical cancer differential expressed genes, adjusted P-value counts, and mean-variance trend. Finally, 50 DEGs were taken from up-regulated as well as 50 from down-regulated from both GSE26511 and GSE41827, and Heatmap was generated (Fig. 2A-C & 3A-C) (Tables 1 & 2).

Functional enrichment analysis

The functional enrichment analysis of the DEGs was done using FUNRICH (Functional enrichment analysis tools) and DAVID enrichment analysis. The genes are divided into various (GO) Gene Ontology which includes Cellular Component (CC), Molecular Function (MF), Biological Process (BP), the biological pathway or the KEGG pathways has all the differential expressed genes which were both up-regulated and down-regulated, based on the threshold of $P< 0.01$ of both the individuals GSE26511 and GSE41827. The GSE26511 has total no of genes for up-regulated Cellular component in Plasma membrane 14 genes, Nucleus 20 genes, Cytosol 8 genes, Cytoplasm 22 genes, Exosomes 7 genes, Extracellular 10 genes for down-regulated Cellular component, Plasma membrane 8 genes, Integral to membrane 3 genes, Nucleus 19 genes, Cytoplasm 16 genes, Exosomes 4 genes, Endoplasmic reticulum 4 genes. Molecular function has datasets for up-regulated genes for Molecular function 9, Cell adhesion molecule activity 3 genes, Transporter activity 4 genes, Transcription regulator activity 3 genes, Receptor activity 2 genes, Transcription factor activity 4 genes and down-regulated molecular function 9 genes, Cell adhesion molecule activity 2 genes, Transporter activity 4 genes, Transcription regulator activity 5 genes, Transcription factor activity 2 genes, Receptor signalling complex scaffold activity 2 genes. Up-regulated Biological process, Cell growth and/or maintenance 4 genes, Transport 6 genes, Cell communication 11 genes, Signal transduction 13 genes, Regulation of nucleobase, nucleoside, nucleotide and nucleic acid metabolism 6 genes down-regulated biological process Protein metabolism 2 genes, Transport 4 genes, Cell communication 12 genes, Signal transduction 12 genes, Regulation of nucleobase, nucleoside, nucleotide and nucleic acid metabolism 10 genes (Suppl. Table 1) (Fig. 4).

The no. of genes in the dataset of GSE41827 for cellular component up-regulated are Nucleus 17 genes, Cytosol 9 genes, Cytoplasm 15 genes,

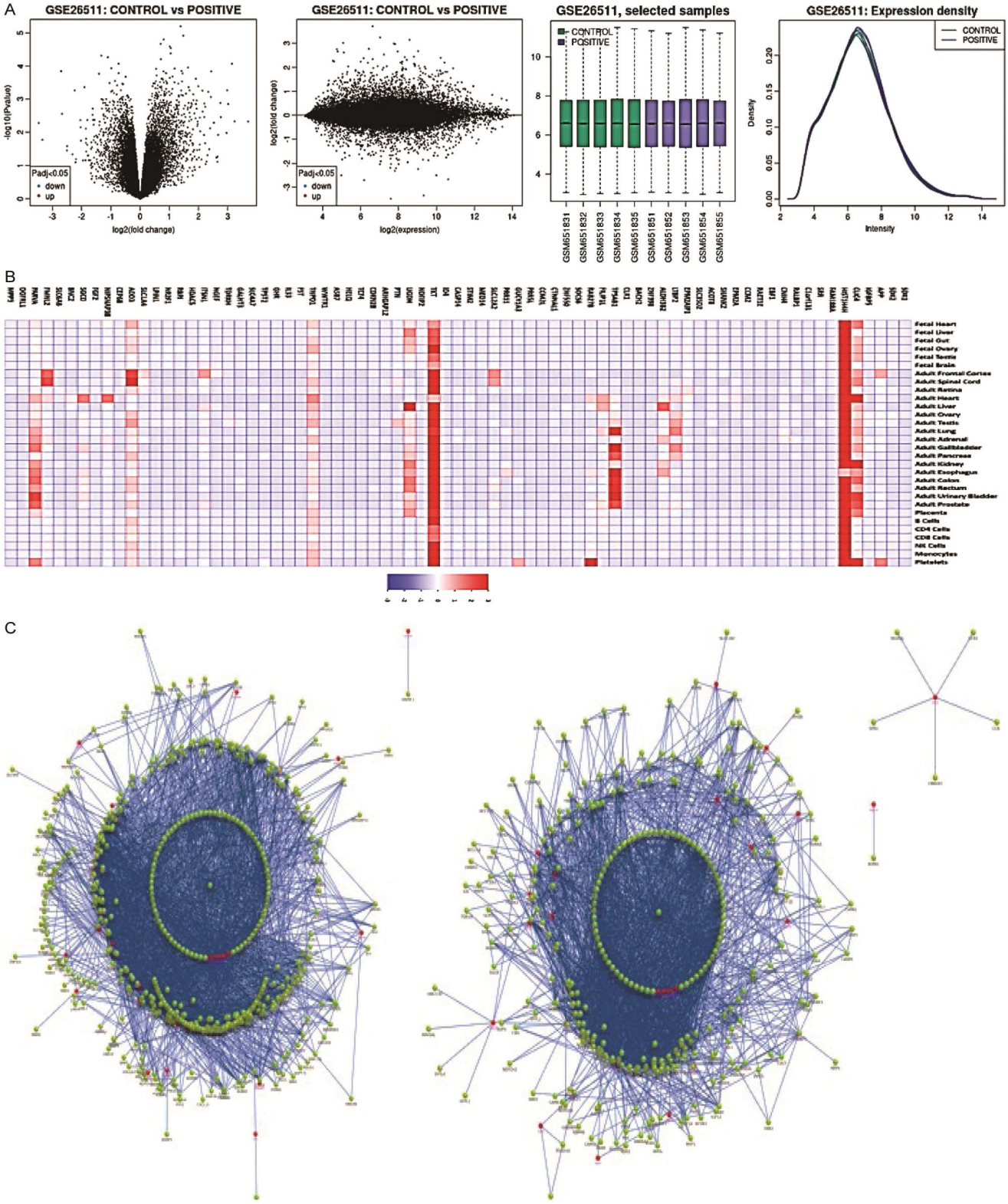

Fig. 2 — The representation of the (A) DEGs in control and cervical cancer; (B) Heatmap showed 100 DEGs based on up-regulated and down-regulated genes in breast cancer; and (C) Presented gene interaction network for both up-regulated and down-regulated gene GSE26511

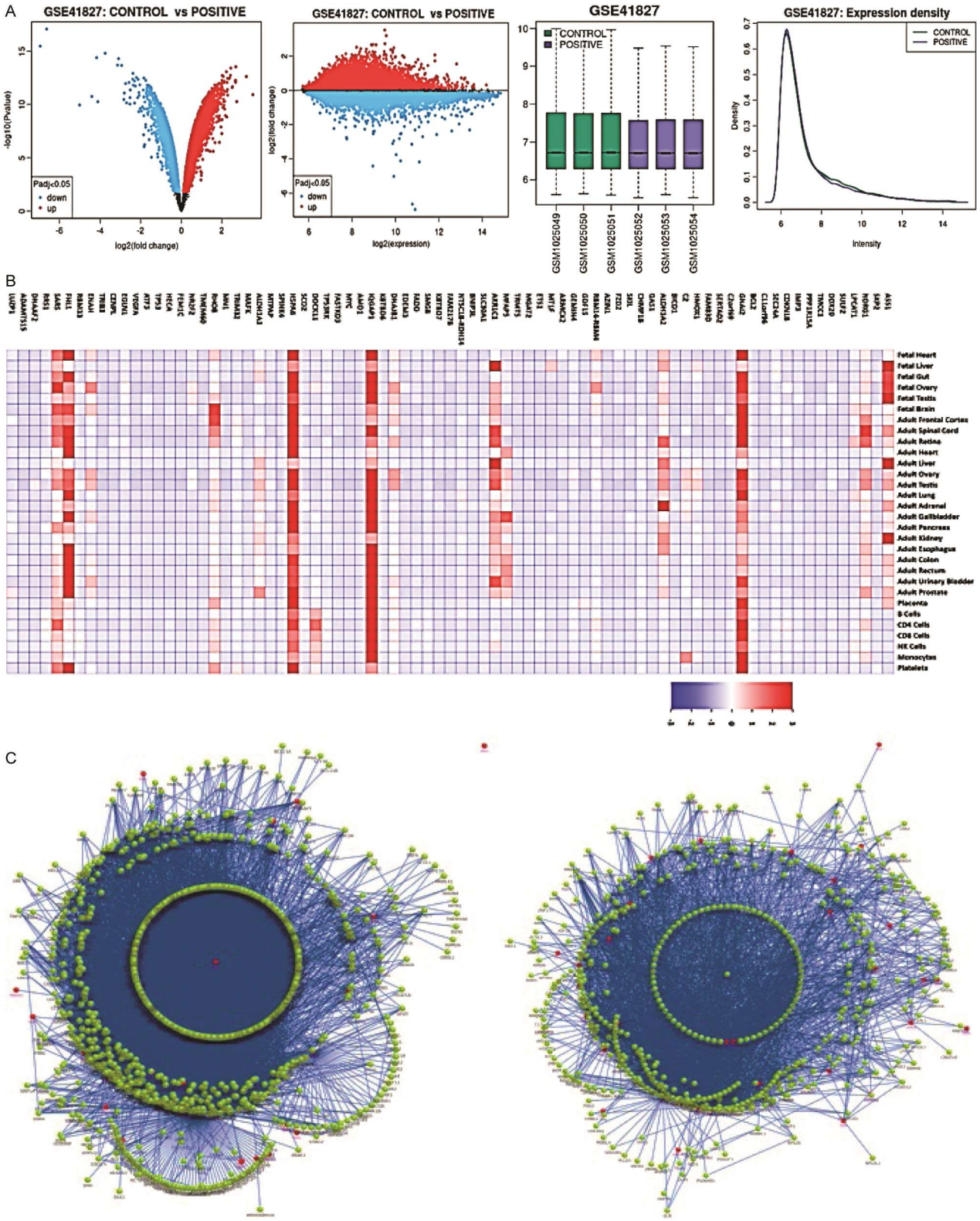

Fig. 3 — The representation of the (A) DEGs in control and cervical cancer; (B) The heatmap showed 100 DEGs based on up-regulated and down-regulated genes in breast cancer; and (C) Presented gene interaction network for both up-regulated and down-regulated gene GSE41827

Table 1 — The DEGs in cervical cancer both up-regulated and down regulated of GSE26511

DEGs	Gene symbol	Log FC
Up-regulated	FBXO5, GEMIN4, LPCAT1, DNAAF2, TRMT5, TMEM203, MYC, FAM83D, CDKN1B, MIR675, GAS1, RHOB, FAM217B, FADD, LUZP1, SKP2, ADAMTS15, TMEM60, MFAP5, MGAT2, TMCC1, SMG8, IMP3, EDEM3, FZD2, SLC35F6, SCO2, FASTKD3, SKP2, KBTBD6, NT5C1B, AMD1, CENPL, TRIM32, C2orf69, HJURP, RRS1, MTPAP, MGAT2, GNAI2, FBXO5, DDX20, FBXL5, MN1, KBTBD7, IQGAP1, ARMCX2, TP53RK, MTPAP, NR2F2	2.68, 2.44, 2.22, 2.42, 2.02, 2.07, 3.2, 2.39, 2.27, 2.34, 2.67, 2, 2.12, 2.67, 2.26, 2.12, 1.87, 2.01, 1.83, 1.97, 1.77, 1.64, 1.69, 1.71, 2.52, 2.02, 1.76, 2, 2.5, 1.95, 1.66, 1.81, 1.51, 1.67, 1.95, 1.77, 1.94, 1.58, 1.97, 1.9, 2.27, 1.8, 1.81, 2.07, 1.53, 1.97, 1.65, 1.6, 1.73, 1.96
Down-regulated	HSPA6, HSPA6, ATF3, HMOX1, SLC30A1, GADD45B, GADD45B, TRIB3, KDM7A, NDRG1, PPP1R15A, ZFAND2A, FEM1C, HSPA1L, DNAJB1, C11orf96, ENAH, SULF2, DNAJB1, EGLN1, PPP1R15A, ALDH3A2, ASS1, LOC10, AKR1C1, BICD1, RBM33, LOC10, CHMP1B, VEGFA, MAFK, RBM14, AZIN1, SERTAD2, SKIL, SPINK4, GADD45B, HECA, ALDH1A3, FHL1, SLC30A1, ETS1, MT1F, AKR1C1, DOCK11, SEC24A, SARS, EGLN1, BNIP3L, GDF15	-6.64, -6.95, -3.75, -4.18, -3.1, -3.14, -2.94, -2.38, -2.22, -1.85, -2.4, -2.13, -1.75, -2.31, -2.57, -2.74, -2.05, -1.69, -2.37, -1.6, -2.26, -1.63, -1.51, -1.51, -1.49, -1.7, -1.55, -1.47, -2.51, -1.87, -1.7, -1.63, -1.48, -1.56, -2.09, -1.73, -2.81, -1.35, -1.32, -1.35, -1.39, -1.73, -1.56, -1.44, -1.45, -1.6, -1.71, -1.51, -1.45, -2.08

Table 2 — The DEGs in cervical cancer both up-regulated and down regulated of GSE41827

DEGs	Gene symbol	Log FC
Up-regulated	SDK2, GHR, ID4, LTBP2, FILIP1L, MIR4683, RNF150, PTN, EBF1, BACH2, PRR5L, PTN, TKT, FILIP1L, ITSN1, TCF4, OGFRL1, FMNL2, GUCY1A3, TPSAB1, FAM188A, CTNNAL1, CLK1, SLC12A2, PARVA, SDK1, RBPJ, MIR4683, SRR, CEP68, UGDH, SLC6A6, FGF2, IGFBP5, ADD3, LOC, TCF4, CLIC4, SLC1A4, WWTR1, APP, ARHGAP12, FST, NR2F1, TCF4, ID4, EPM2AIP1, SLC4A7, IL33, TNPO1	1.387, 1.484, 0.813, 0.701, 1.018, 1.044, 0.715, 3.147, 1.646, 1.184, 1.426, 2.443, 0.801, 0.879, 0.893, 1.459, 0.571, 1.11, 1.02, 0.752, 0.762, 1.912, 0.731, 0.782, 0.883, 1.434, 0.684, 1.182, 0.816, 0.919, 1.313, 0.916, 0.607, 1.9940.732, 0.683, 1.666, 0.731, 0.602, 1.102, 0.889, 0.751, 2.988, 1.697, 1.408, 2.139, 0.837, 0.989, 2.335, 0.645
Down-regulated	ADGRF4, LINC01503, RAET1E, NR2F1-AS1, ADGRF4, SOCS6, CDKN2B, HDAC5, GALNT3, CCM2L, BORA, RBPJ, SGCD, C1orf131, SOCS6, CNIH4, SGCD, LOC1, ZNF550, ACOT8, CDKN2B, PRR11, TPST2, NDFIP2, BNC2, HIST1, MIR6716, LPIN1, ID2-AS1, MED14, HELQ, MPP5, RALBP1, BNC2, ASB7, CNIH4, MIR21, ALDH3B2, SLC35D2, RAB27B, SHANK2, HIST1, ZNF398, STIM2, NIPSNAP3B, CASP14, TDRKH, NGEF, SLC25A43, HIST1H4H	-1.33, -1.102, -0.985, 0.545, -2.708, -0.731, -1.406, -0.495, -0.863, 0.542, -1.041, 0.505, 0.463, -0.609, -0.584, -0.784, 0.426, -1.912, 0.53, -0.659, -2.243, -0.954, -0.993, -0.9, 0.42, -0.805, 0.521, 0.528, -0.426, -0.451, 0.416, -0.585, -0.401, 0.499, -0.412, -0.673, -0.614, -1.156, -0.318, -1.315, -1.309, -0.702, -0.498, 0.309, 0.365, -1.27, -0.6, -0.358, -0.931, -0.76

Exosomes 5 genes, Endoplasmic reticulum 5 genes, Extracellular 5 genes, Cellular component down-regulated Plasma membrane 4 genes, Nucleus 20 genes, Cytosol 8 genes, Cytoplasm 22 genes, Endoplasmic reticulum 9 genes, Extracellular 6 genes. The total genes for Molecular function up-regulated are Transcription regulator activity 2 genes, Transcription factor activity 2 genes, Ubiquitin-specific protease activity 2 genes, GTPase activity 2 genes, Ribonucleoprotein 2 genes down-regulated Molecular function unknown 10 genes, Transporter activity 4 genes, Catalytic activity 6 genes, Transcription factor activity 3 genes, RNA binding 2 genes, Heat shock protein activity 2 genes. Biological function up-regulated genes for Metabolism 5, Energy pathways 4, Cell communication 11 genes, Signal transduction 11 genes, Regulation of nucleobase, nucleoside, nucleotide and nucleic acid metabolism 6 genes for down-regulated biological process 8 genes for Metabolism, Energy pathways 7 genes, Transport 5 genes, Cell communication 8 genes, Signal transduction 9 genes, Regulation of nucleobase, nucleoside, nucleotide and nucleic acid metabolism 5 genes (Suppl. Table 2) (Fig. 5).

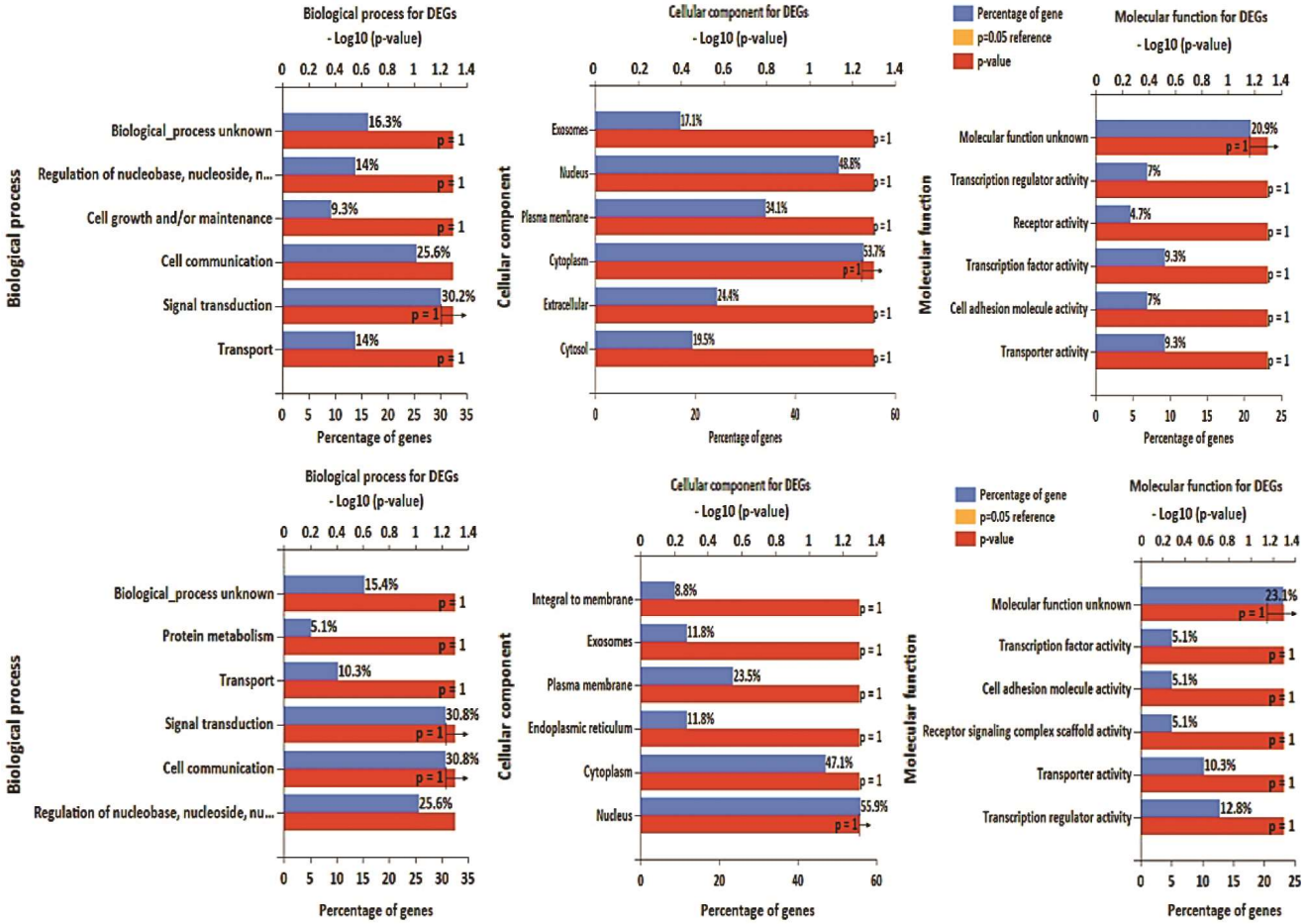

Fig. 4. — DEGs, differentially expressed genes of both up-regulated and down-regulated; Biologic processes (BP); Gene Ontology (GO);Cellular components (CC); and Molecular functions (MF) for GSE26511

KEGG Pathway analysis

The KEGG pathway of up-regulated DEGs of GSE26511 gained Transmembrane transport of small molecules, Transport of inorganic cations/anions and amino acids/oligopeptides, SLC-mediated transmembrane transport, Glypican pathway, Proteoglycan syndecan-mediated signaling events and for down-regulated Syndecan-1-mediated signaling events, Regulation of CDC42 activity, Glypican pathway, GMCSF-mediated signaling events, CDC42 signaling events, Signaling events mediated by Hepatocyte Growth Factor Receptor (c-Met) (Suppl. Table 3 & Fig.6).

The KEGG pathway of up-regulated DEGs of GSE41827 are Metabolism, Syndecan-1-mediated signaling events, Glypican pathway, TRAIL signaling pathway, Sphingosine 1-phosphate (S1P) pathway, Proteoglycan syndecan-mediated signaling events and Syndecan-1-mediated signaling events, Glypican pathway, GMCSF-mediated signaling events, Nectin adhesion pathway, TRAIL signaling pathway, IGF1 pathway for down-regulated (Suppl. Table 4 & Fig. 7).

PPI interaction

The protein-protein interaction (PPI) network for the DEGs was visualized and constructed using the StringApp. The Cytohubba available in the Cytoscape Rank the top 6 genes according to the MCC rank method, the top 6 genes for the GSE26511 are ID2, FGF2, CLIC4, MED14, NGEF, TCF4. Mainly involved in the pathway such as Syndecan-1-mediated signaling events, Glypican pathway, CDC42 signaling events, Glypican 1 network. The top 6 genes for GSE41827 are ATF3, BCL2, MAF, MYC, TP53, HMOX and the pathway involved are GMCSF-mediated signaling events, Glypican pathway, GMCSF-mediated signaling events, Proteoglycan syndecan-1-mediated signaling events, TRAIL signaling pathway, Nectin adhesion pathway (Figs. 8-11) (Tables 3 & 4).

Molecular descriptors (MDs)

The low values of TPSA and MW mean that molecules easily cross membranes.All molecules have a TPSA lower than 450, it means that molecules easily cross membranes. The number values of OH-N or O-NH interactions are 5 less, so there is no Lipinski's, Veber's or Igan's violations. The FDA approved standard drugs have excellent oral bioavailability and absorption, as observed. The current study revealed that four compounds satisfy all Lipinski's requirements; however, Molinspiration study shows the lipophilicity, solubility, bioavailability, and various physicochemical characteristics, enabling us to rank compounds for additional experimental validation (Table 5 and Suppl. Table 5).

ADMET evaluation

Swiss ADMET assesses compounds based on oral bioavailability, GI absorption, BBB permeation, CYP1A2 inhibitor, CYP2C19 inhibitor, P-gp substrate, CYP2D6 inhibitor, CYP3A4 inhibitor, CYP2C9 inhibitor, and Log Kp (skin permeation) to determine the most effective molecule. The results of ADMET prediction show that almost all of the selected compounds have good ADMET properties, as shown in (Suppl. Tables 6 & 7).

Brain and intestinal estimated (BOILED-Egg)

The BOILED Egg model possess the white area reflects the possibility of gastrointestinal absorption and the yellow yolk represents the capacity to cross the blood-brain barrier. For the Drug 5-flurouracil and Gemcitabine when did the Brain and Intestinal Estimation the drug showed absorption in gastrointestinal but not have capacity to cross the blood-brain barrier[33] (Fig. 12).

Molecular docking

Auto Dock Vina was used for virtual screening, and the receptor and ligand PDB formats were converted into PDBQT files. The grid box parameters for each receptor are listed ina grid

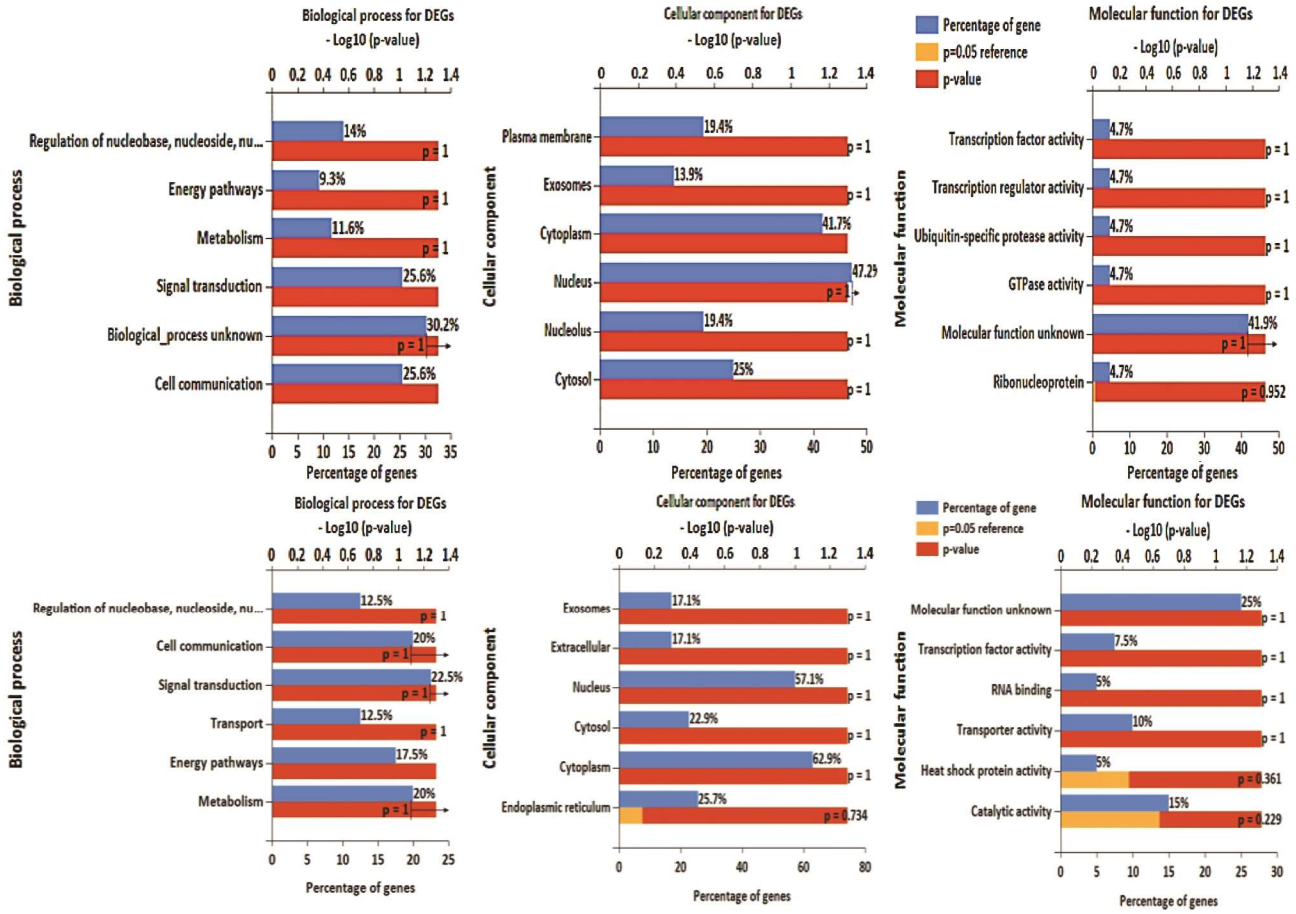

Fig. 5 — DEGs, differentially expressed genes of both up-regulated and down-regulated ; Biologic processes (BP); Gene Ontology (GO); Cellular components (CC); Molecular functions (MF) for GSE41827

Table 3 — Identified top hub genes by PPI interactions

Gene	No. of Nodes	No. of edges	avg. local clustering coefficient	PPI enrichment p-value
ID2	11	29	0.814	6.42e-06
FGF2	11	31	0.717	7.16e-06
CLIC4	11	20	0.902	0.00476
MED14	11	55	1	<1.0e-16
NGEF	11	49	0.931	3.24e-12
TCF4	11	37	0.822	1.07e-08

Table 4 — Identifiedtop hub genes by PPI interactions.

Gene	No. of Nodes	No. of edges	Avg. local clustering coefficient	PPI enrichment p-value
ATF3	11	43	0.872	3.12e-10
BCL2	11	52	0.953	1.11e-15
MAF	11	26	0.857	0.000756
MYC	11	30	0.729	0.00895
TP53	11	46	0.91	4.66e-06
HMOX	11	23	0.802	0.00274

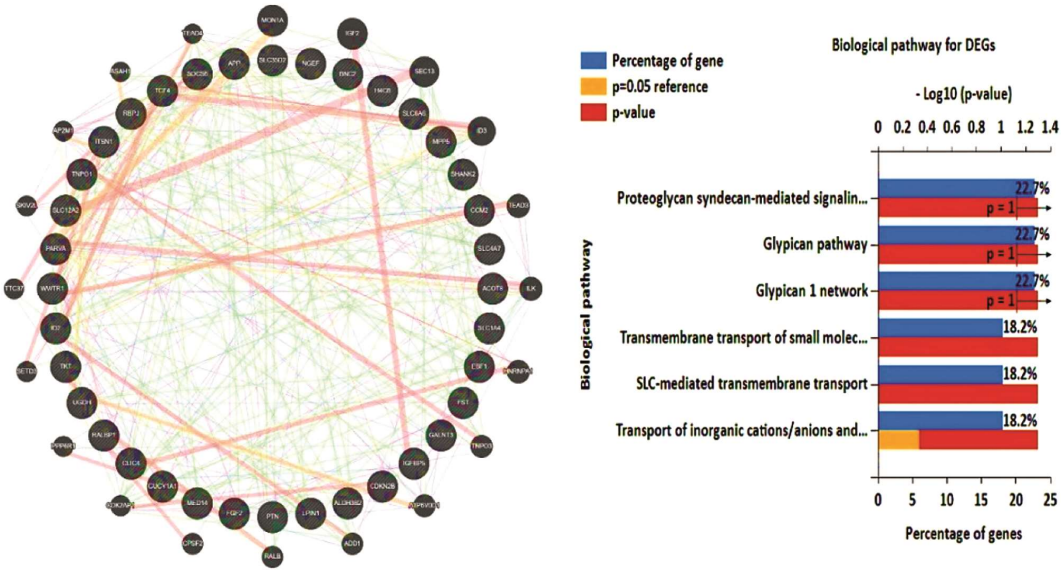

Fig. 6 — KEGG pathway hub genes analysis and biological pathway were achieved using the David enrichment analysis tool for GSE26511

file generated a ligand log file, which was then used to run the docking score in Cygwin. Once an exhaustiveness score of ten was obtained, validation was carried out. The findings were calculated using the PyMOL result of the protein-ligand complex, which is based on the binding energy and activation of hydrogen bonds formed by active amino acids. The ligand-protein interactions were viewed in 2D and 3D using the BIOVIA Discovery Studio Visualizer, LigPlot+, and Proteins Plus. In this work, the selected biomarkers from GSE26511 are ID2, FGF2, CLIC4, MED14, NGEF, TCF4 docked against the FDA approved drugs, 5-flurouracil and Gemcitabine already present for cervical cancer to determine their binding affinity and ATF3, BCL2, MAF, MYC, TP53, HMOX from GSE41827. Detailed information regarding the interactions between chosen receptor amino acid residues and ligands is provided. The docking scores of the ligands against the receptors employed in the study are also been provided. (Suppl. Tables 8-11).

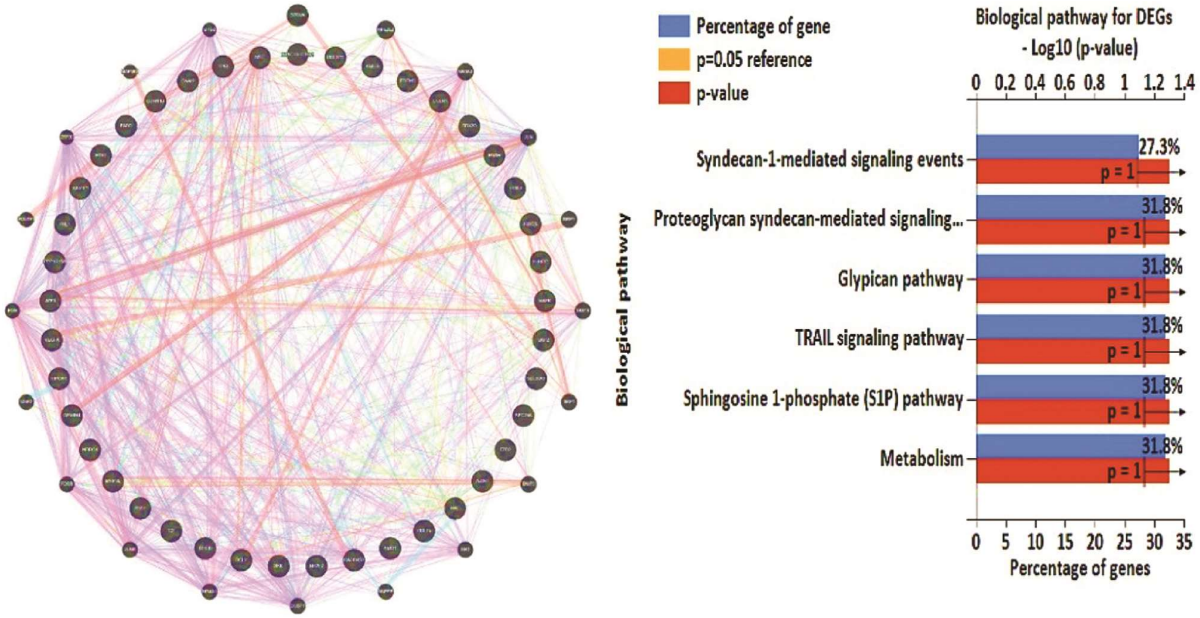

Fig. 7 — KEGG pathway hub genes analysis and biological pathway were achieved using the David enrichment analysis tool GSE41827

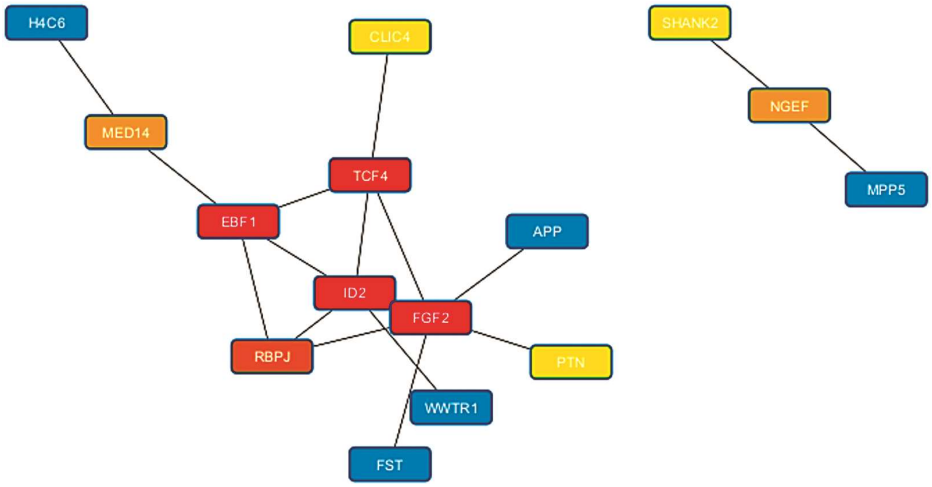

Fig. 8 — The picture above shows the top 6 hub genes set obtained from Cytoscape of GSE26511

Screening of Drugs with GSE26511 receptor ID2 (PDB id: 1K17)

The drugs show the good binding efficiency with the receptor ID2 which was -5.2 (kcal/mol) for 5-flurouracil and -5.5 (kcal/mol)with Gemcitabine. The ID2 with binding efficiency of -5.2 (kcal/mol) showed four hydrogen bonds interaction with the amino acid Gly 28, Glu38, Ser29, Asp 31 (bond lengths of 2.01 Å, 2.19Å, 2.33 Å, 2.67Å, respectively) and the binding with Gemcitabine showed single hydrogen bond interaction with amino acid Gln 59 with bond length of 2.24 Å (Table 6 & Fig. 13).

Screening of Drugs with GSE26511 receptor CLIC4 (PDB id: 3OQS)

The drugs show the binding efficiency with the receptor CLIC4 which was -6.1 (kcal/mol) for 5-flurouracil and -7.2 (kcal/mol) with Gemcitabine. The CLIC4 with binding efficiency of -6.1 (kcal/mol) showed two hydrogen bonds interaction with the amino acid His30 and Ser33 with bond length of 2.05 Å and 2.08 Å whereas, the binding with Gemcitabine showed 5 hydrogen bond interaction with amino acid Asn209, Ser33, Trp212, His30, Trp254 with bond length of (2.27 Å, 2.71 Å, 2.89 Å, 2.98 Å, 3.34 Å, respectively) (Table 7 & Fig. 14).

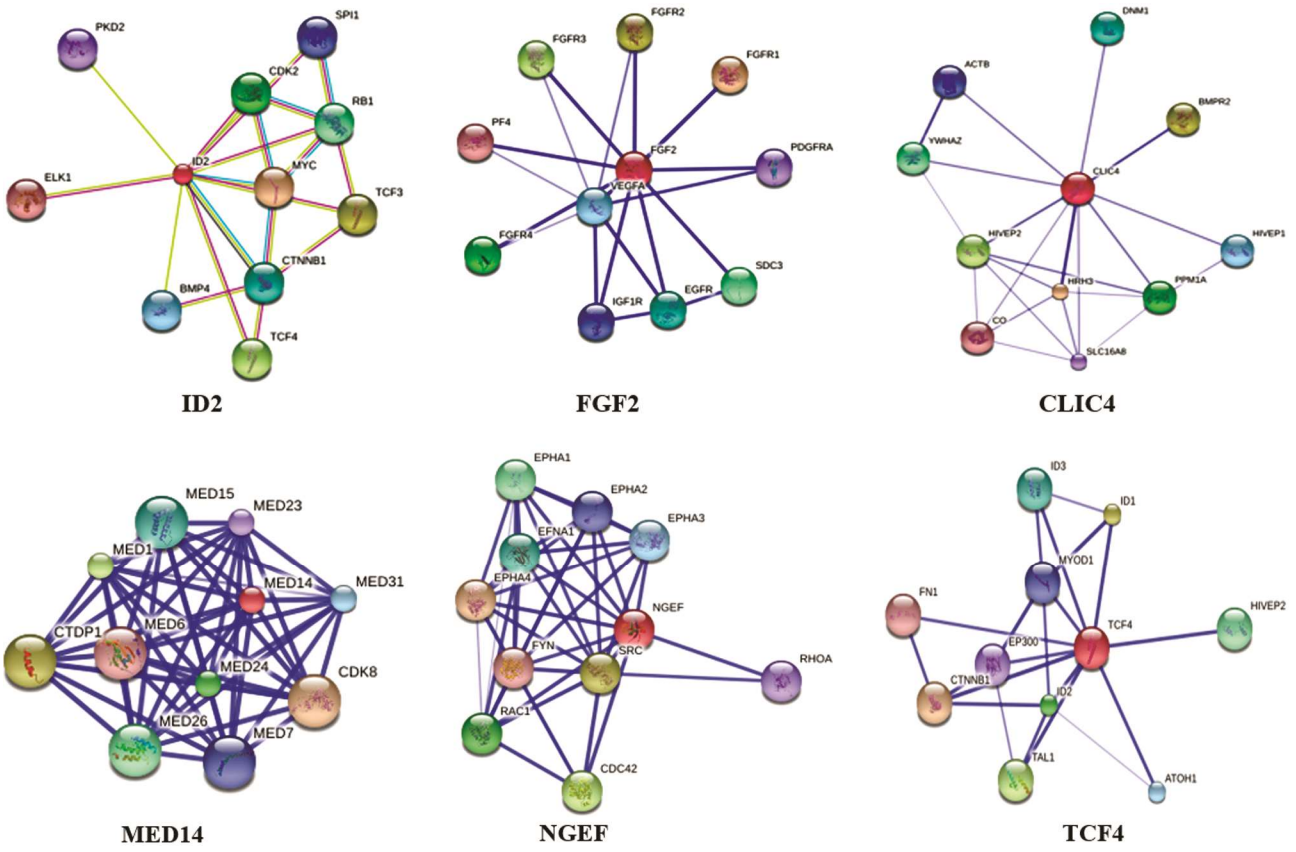

Fig. 9 — The representation of the top 6 most significant hub genes identified from the PPI network, utilizing the CytoHubba plugin and ranked by the MCC method within Cytoscape of GSE26511

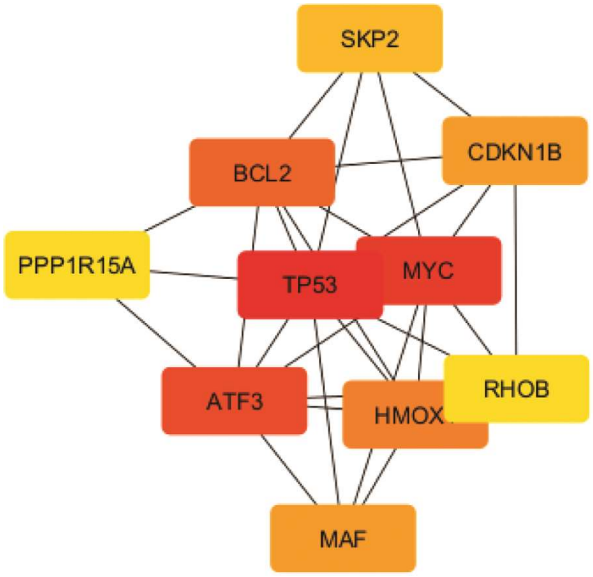

Fig 10 — The picture above shows the top 6 hub genes set obtained from Cytoscapeof GSE41827

Screening of Drugs with GSE26511 receptor NGEF (PDB id: 2ZOQ)

The drugs show the binding efficiency with the receptor NGEF which was -6.0 (kcal/mol) for 5-flurouracil and same -6.0 (kcal/mol) with Gemcitabine. The NGEF with binding efficiency of -6.0 (kcal/mol) showed 4 hydrogen bonds interaction with the amino acid Tyr209, Glu59, Gln62, Leu267 with bond length of (2.14 Å, 2.20 Å, 2.55 Å, 2.68 Å respectively) whereas, the binding with Gemcitabine showed 5 hydrogen bond interaction with amino acid Arg259, Ala260, His247, Glu237, Lys 245 with bond length of (2.06 Å, 2.13 Å, 2.27 Å, 2.46 Å, 3.32 Å, respectively) (Table 8 & Fig. 14).

Screening of Drugs with GSE26511 receptor TCF4 (PDB id: 1JPW)

The drugs show the binding efficiency with the receptor TCF4 which was -6.0 (kcal/mol) for 5-flurouracil and same -6.2 (kcal/mol) with Gemcitabine. The TCF4 with binding efficiency of -6.0 (kcal/mol) showed 5 hydrogen bonds interaction with the amino acid Arg339, Asn386, Ser343 Arg385, Glu438 with bond length of (2.05 Å, 2.16 Å, 2.22 Å, 2.55 Å, 2.79 Å, respectively) whereas, the binding with Gemcitabine also showed

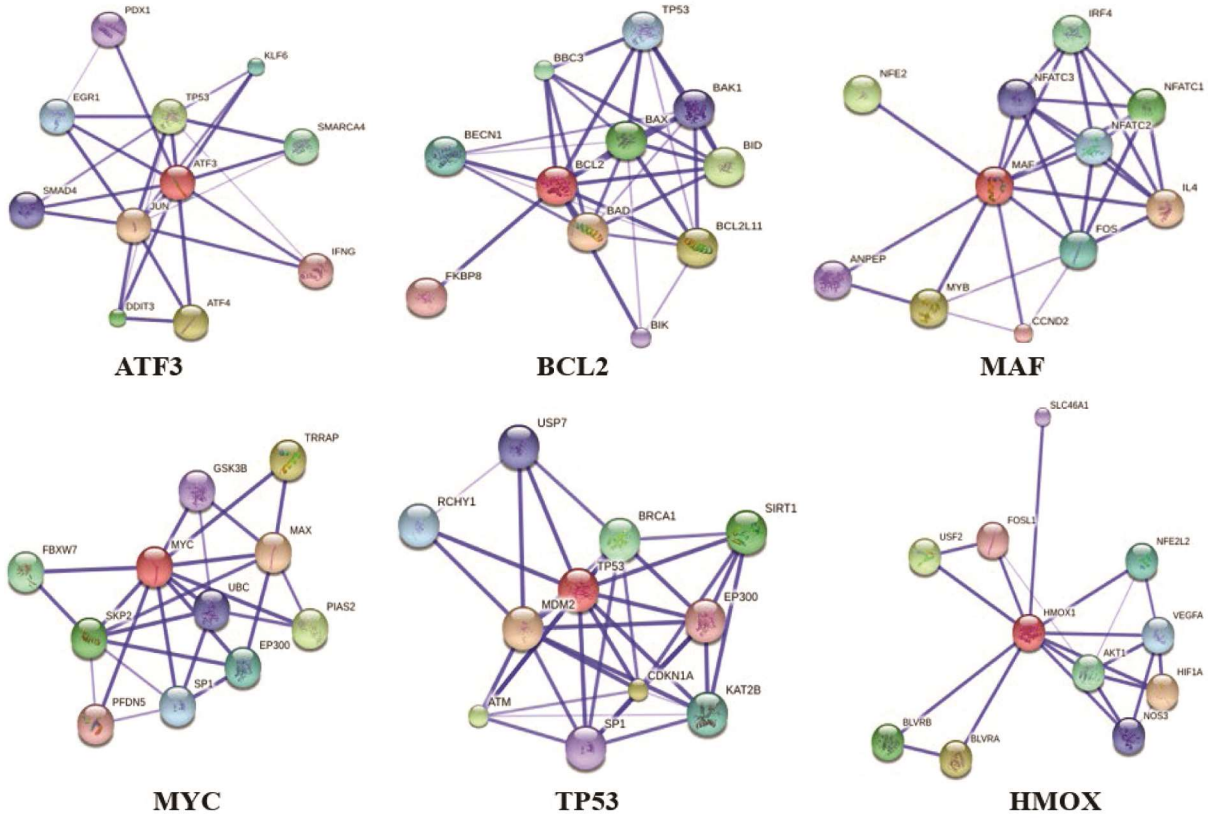

Fig. 11 — The representation of the top 6 most significant hub genes identified from the PPI network, utilizing the CytoHubba plugin and ranked by the MCC method within Cytoscape of GSE41827

Table 5 — Analysis of Lead likeness, Lipinski Ro5, Veber, Egan, and Ghose for phytochemicals and reference drugs

Standards	Drug likeness					Medicinal chemistry alerts		
	Lipinski	Ghose	Veber	Egan	Muegge	PAINS (Pan Assay Interference Structures)	Brenk	Lead likeness
5-flurouracil	0	1	0	0	0	0	0	1
Gemcitabine	0	1	0	0	0	0	0	0

Table 6 — Docking score and interacting residues of selected drugs with ID2

Compound	Type of bond	Binding affinity (kcal/mol)	Amino acid	Bond length Å
5-flurouracil	H-bond	-6.1	His30	2.05
	H-bond		Ser33	2.08
	Pi alkyl		Trp212	4.38
Gemcitabine	H-bond	-7.2	Asn209	2.27
	H-bond		Ser33	2.71
	H-bond		Trp212	2.89
	H-bond		His30	2.98
	H-bond		Trp254	3.34

5 hydrogen bond interaction with amino acid Lys378, Ser343, Arg385, Glu438 with bond length of (2.08 Å, 2.39 Å, 2.66Å, 3.09 Å, 3.13 Å respectively) (Table.9 & Fig. 15).

3.8.6. Screening of Drugs with GSE41827 receptor MAF (PDB id: 1EX2)

The drugs show the binding efficiency with the receptor MAF which was -6.9 (kcal/mol) for 5-

Table 7 — Docking score and interacting residues of selected drugs with CLIC4

Compound	Type of bond	Binding affinity (kcal/mol)	Amino acid	Bond length Å
5-flurouracil	H-bond	-5.2	Gly 28	2.01
	H-bond		Glu38	2.19
	H-bond		Ser29	2.33
	H-bond		Asp 31	2.67
Gemcitabine	H-bond	-5.5	Gln 59	2.24

Table8 — Docking score and interacting residues of selected drugs with NGEF

Compound	Type of bond	Binding affinity (kcal/mol)	Amino acid	Bond length Å
5-flurouracil	H-bond	-6.0	Tyr209	2.14
	H-bond		Glu59	2.20
	H-bond		Gln62	2.55
	H-bond		Leu267	2.68
	Pi alkyl		Leu121	4.68
Gemcitabine	H-bond	-6.0	Arg259	2.06
	H-bond		Ala260	2.13
	H-bond		His247	2.27
	H-bond		Glu237	2.46
	H-bond		Lys245	3.32

Table9 — Docking score and interacting residues of selected drugs with TCF4

Compound	Type of bond	Binding affinity (kcal/mol)	Amino acid	Bond length Å
5-flurouracil	H-bond	-6.0	Arg339	2.05
	H-bond		Asn386	2.16
	H-bond		Ser343	2.22
	H-bond		Arg385	2.55
	H-bond		Glu438	2.79
Gemcitabine	H-bond	-6.2	Lys378	2.08
	H-bond		Ser343	2.39
	H-bond		Asn386	2.66
	H-bond		Arg385	3.09
	H-bond		Gly382	3.13

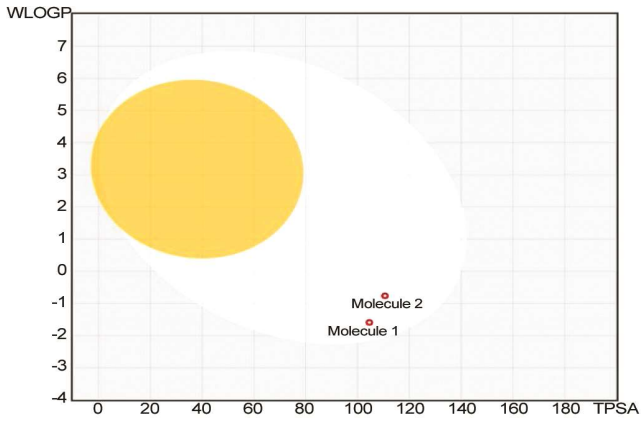

Fig. 12 — Representation of the BOILED Egg model. Molecule 1: 5-flurouracil; 2: Gemcitabine

flurouracil and -6.7 (kcal/mol) with Gemcitabine. The MAF with binding efficiency of -6.9 (kcal/mol) showed three hydrogen bonds interaction with the amino acid Arg14, Lys53, Ala8 with bond length of 2.41 Å, 2.61 Å, 2.86 Å whereas, the binding with Gemcitabine showed four hydrogen bond interaction with amino acid Arg14, Gln10, Ser11, Ser9 with bond length of 2.01 Å, 2.22 Å, 2.36 Å, 2.94 Å respectively) (Table.10 & Fig. 16 & 17).

Screening of Drugs with GSE41827 receptor MYC(PDB id: 2ORB)

The drugs showed good binding efficiency with the receptor MYC which was -5.6 (kcal/mol) for 5-flurouracil and -5.8 (kcal/mol) with Gemcitabine. The MYC with binding efficiency of -5.6 (kcal/mol) showed five hydrogen bonds

Table 10 — Docking score and interacting residues of selected drugs with MAF

Compound	Type of bond	Binding affinity (kcal/mol)	Amino acid	Bond length Å
5-flurouracil	H-bond	-6.9	Arg14	2.41
	H-bond		Lys53	2.61
	H-bond		Ala8	2.86
	Pi alkyl		Val29	5.03
Gemcitabine	H-bond	-6.7	Arg14	2.01
	H-bond		Gln10	2.22
	H-bond		Ser11	2.36
	H-bond		Ser9	2.94

Table11 — Docking score and interacting residues of selected drugs with MYC

Compound	Type of bond	Binding affinity (kcal/mol)	Amino acid	Bond length Å
5-flurouracil	H-bond	-5.6	Tyr177	1.99
	H-bond		Tyr144	2.14
	H-bond		Ser10	2.45
	H-bond		Lys146	2.46
	H-bond		Lys107	2.48
	Pi alkyl		Ala12	4.46
Gemcitabine	H-bond	-5.8	Ser10	2.29
	H-bond		Lys203	2.45
	H-bond		Tyr144	2.48
	H-bond		Tyr177	2.73

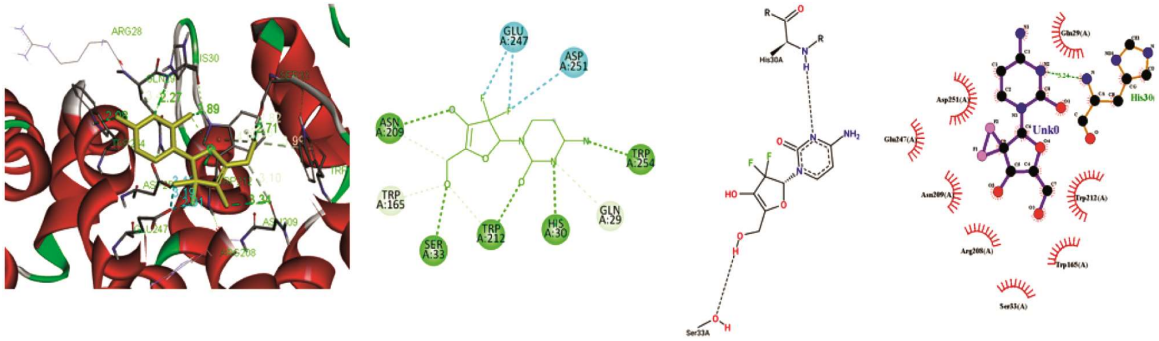

Fig. 13 — 2D, 3D, and Lig plot docking pose of ID2-Gemcitabine complex

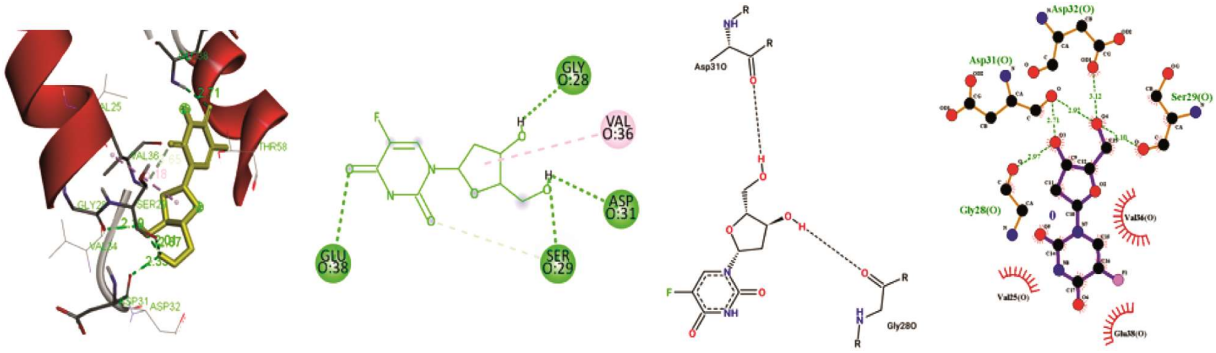

Fig. 14 — 2D, 3D, and Lig plot docking pose of CLIC4-5-flurouracil complex

interaction with the amino acid Tyr177, Tyr144, Ser10, Lys146, Lys107 with bond length of (1.99 Å, 2.41 Å, 2.45 Å, 2.46 Å, 2.48 Å) whereas, the binding with Gemcitabine showed four hydrogen bond interaction with amino acid Ser10, Lys203, Tyr144, Tyr177 with bond length of 2.29 Å, 2.45 Å, 2.48 Å, 2.73 Å respectively) (Table.11 & Fig.18).

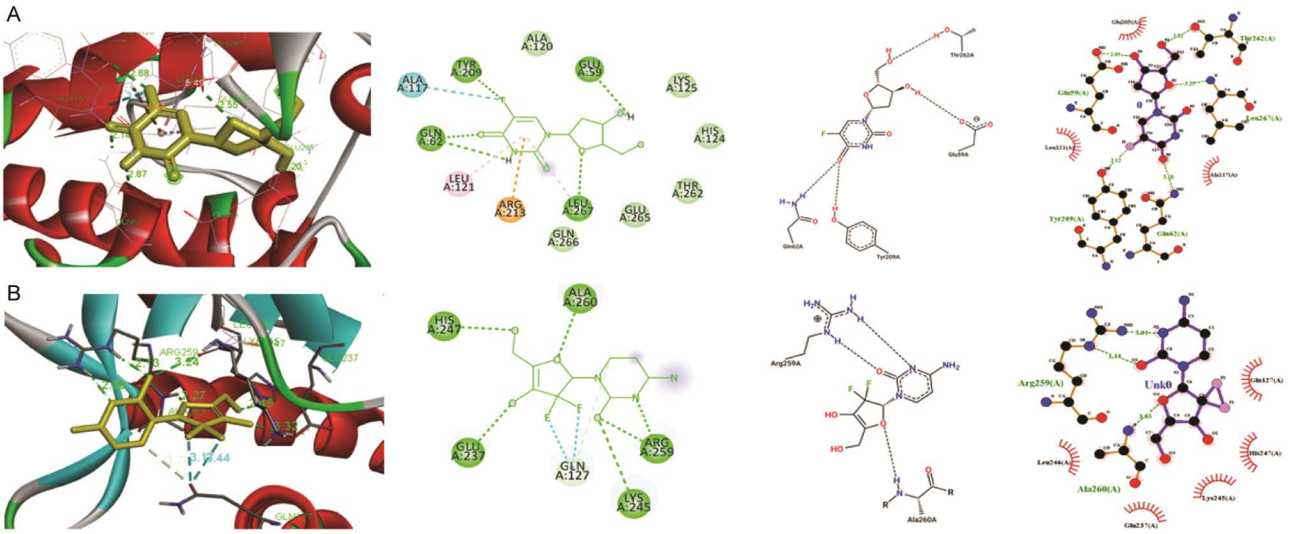

Fig. 15 — 2D, 3D, and Lig plot docking pose of NGEF-ligand complex (A) 5-flurouracil; and (B) Gemcitabine

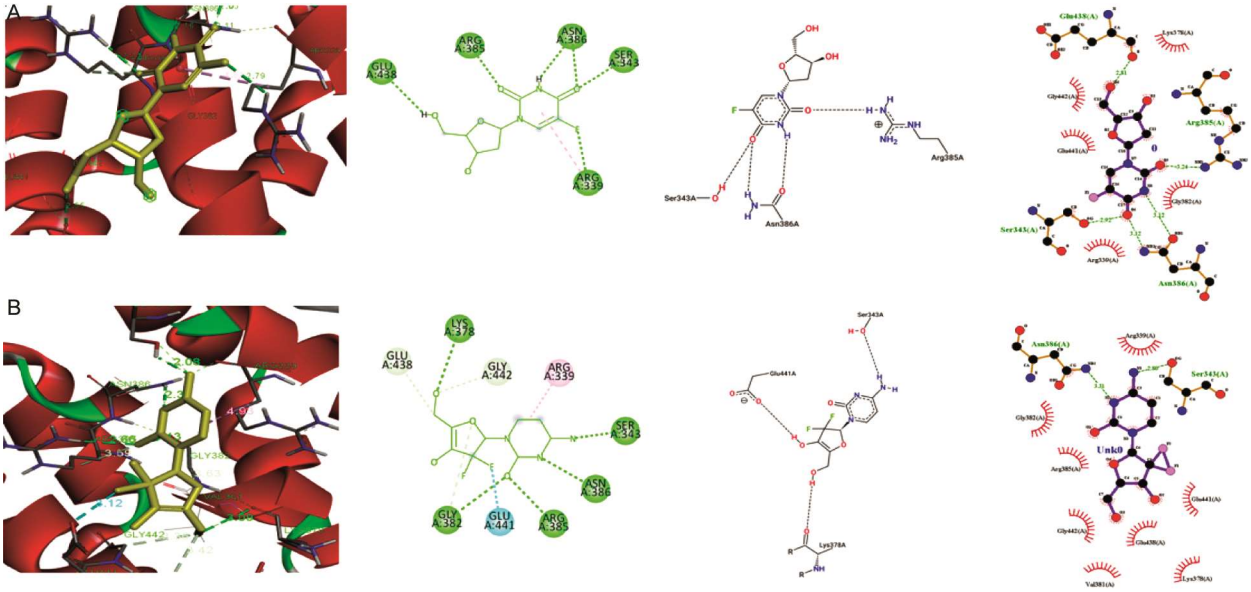

Fig. 16 — 2D, 3D, and Lig plot docking pose of TCF4-ligand complex (A) 5-flurouracil; and (B) Gemcitabine

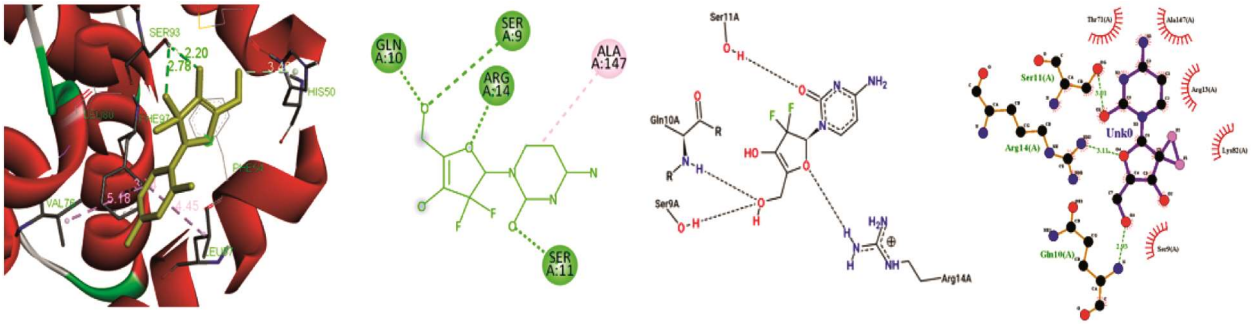

Fig. 17 — 2D, 3D, and Lig plot docking pose of MAF Gemcitabine complex

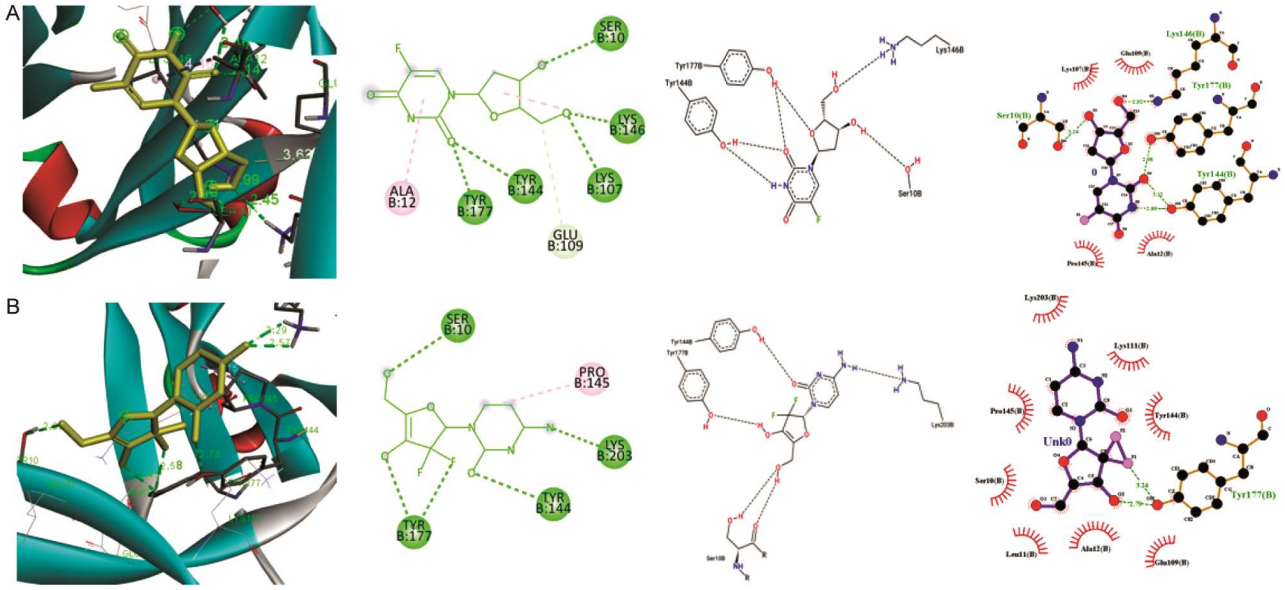

Fig. 18 — 2D, 3D, and Lig plot docking pose of MYC -ligand complex (A) 5-flurouracil; and (B) Gemcitabine

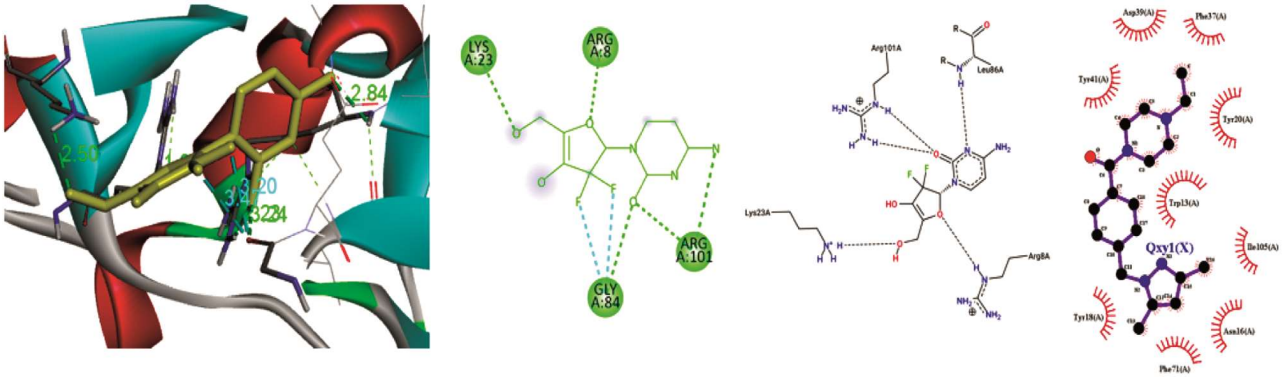

Fig. 19 — 2D, 3D, and Lig plot docking pose of TP53-Gemcitabine complex

Table12— Docking score and interacting residues of selected drugs with TP53

Compound	Type of bond	Binding affinity (kcal/mol)	Amino acid	Bond length Å
5-flurouracil	H bond	-5.6	Lys23	1.97
	H bond		Arg101	2.23
	H bond		Leu86	2.77
Gemcitabine	H bond	-5.8	Lys23	1.94
	H bond		Arg8	2.23
	H bond		Arg101	2.50
	H bond		Gly84	3.24

Screening of Drugs with GSE41827 receptor TP53(PDB id:9CKJ)

The drugs show the binding efficiency with the receptor TP53 which was -5.6 (kcal/mol) for 5-flurouracil and -5.8 (kcal/mol) with Gemcitabine. The TP53 with binding efficiency of -5.6 (kcal/mol) showed three hydrogen bonds interaction with the amino acid Lys23, Arg101, Leu86 with bond length of (1.97 Å, 2.23 Å, 2.77 Å) whereas, the binding with Gemcitabine showed four hydrogen bond interaction with amino acid Lys23, Arg8, Arg101, Gly84 with bond length of 1.94 Å, 2.23 Å, 2.50 Å, 3.24 Å respectively) (Table.12 & Fig.19).

Conclusion

The objective of the study was to find out the hub genes and the signalling pathways associated with the cervical cancer and carry out the molecular docking

studies and finding out the efficacy of the drugs with the hub proteins. Using the computational techniques and the evaluation of the biological data available it was used to identify the protein crucial in the Cervical cancer signalling pathways. The Gene Expression Omnibus (GEO) analysis gave 239 genes for GSE26511 and 248 genes for GSE41827 which included 145 up-regulated and 94 down-regulated for GSE26511 and 174 up-regulated, 74 down-regulated for GSE41827. By the construction of protein- protein interaction network (PPI) of the DEGs for both GSE26511 and GSE41827 we got 6 hub genes for GSE26511 (ID2, FGF2, CLIC4, MED14, NGEF, TCF4) and 6 hub genes for GSE41827 which are (ATF3 BCL2, MAF, MYC, TP53, HMOX). Finally, we have taken 2 FDA approved drugs named 5-flurouracil and Gemcitabine inhibitors for the cervical cancer and did the molecular docking studies for the HUB protein which were 12 in number selected from both GSE41827 and GSE26511. The molecular analysis studies revealed that out of 6 hub genes selected from GSE26511, ID2 showed good binding affinity of -5.2 with drug 5-flurouracil, CLIC4 with Gemcitabine with binding affinity of -7.2 and 5 hydrogen bonds MED14 with 5-flurouracil binding affinity of -6.5 whereas NGEF as well as TCF4 both showed good binding affinity with both the drugs. The HUB protein named MAF from GSE41827 showed binding affinity of -6.7 with Gemcitabine including 4 hydrogen bonds. MYC with both the drugs showed good binding affinity and TP53 showed binding affinity of -5.6 with 5-flurouracil but increased hydrogen bonds with Gemcitabine. So finally, it can be concluded that the HUB protein from the GSE26511 showed good binding affinity with both the drugs as compared to the HUB proteins of GSE41827.

Acknowledgement

The authors extent their appreciation to the Researchers Supporting Program for funding this work through Researchers Supporting Project No. (RSP2025R371) - King Saud University, Riyadh, Saudi Arabia. Authors also thank REVA University for providing all necessary facilities.

Conflict of interest

All authors declare no conflict of interest.

References

1 Elias MH, Das S & Abdul Hamid N, Candidate genes and pathways in cervical cancer: a systematic review and integrated bioinformatic analysis. *Cancers,* 15 (2023) 853.

2 Podwika SE & Duska LR, Top advances of the year: cervical cancer. *Cancer*, 129 (2023) 657.

3 Chen Q, Hu J, Sun X & Long W, Transcriptome sequencing reveals pathways and genes dysregulated in HPV infected cervical cancer. *Eur J Gynaecol Oncol*, 41 (2020) 996.

4 Li C, Liu D, Yang S & Hua K, Integrated single-cell transcriptome analysis of the tumor ecosystems underlying cervical cancer metastasis. *Front Immunol*, 13 (2022) 966291.

5 Liang B, Li Y & Wang TA, A three miRNAs signature predicts survival in cervical cancer using bioinformatics analysis. *Sci Rep,* 7 (2017) 5624.

6 Ogasawara, A & Hasegawa K, Recent advances in immunotherapy for cervical cancer. *Int J Clin Oncol,* 30 (2025) 434.

7 ShornaleAkter M, Uddin MH, Atikur Rahman S, Hossain MA, Ashik MA, Zaman NN, Faruk O, Hossain MS, Parvin A & Rahman MH, Transcriptomic analysis revealed potential regulatory biomarkers and repurposable drugs for breast cancer treatment. *Cancer Rep*, 7 (2024) e2009.

8 Dai F, Chen G, Wang Y, Zhang L, Long Y, Yuan M, Yang D, Liu S, Cheng Y & Zhang L, Identification of candidate biomarkers correlated with the diagnosis and prognosis of cervical cancer *via* integrated bioinformatics analysis. *Onco Targets Ther*, (2019) 4517.

9 Clough E, Barrett T, Wilhite SE, Ledoux P, Evangelista C, Kim IF, Tomashevsky M, Marshall KA, Phillippy KH, Sherman PM & Lee H, NCBI GEO: archive for gene expression and epigenomics data sets: 23-year update. *Nucleic Acids Res*, 52 (2024) D138.

10 Yang HJ, Xue JM, Li J, Wan LH & Zhu YX. Identification of key genes and pathways of diagnosis and prognosis in cervical cancer by bioinformatics analysis. *Mol Genet Genomic Med,* 8 (2020) e1200.

11 Kumar US, Kumar TD, Bithia R, Sankar S, Magesh R, Sidenna M, Doss GPC & Zayed H, Analysis of differentially expressed genes and molecular pathways in familial hypercholesterolemia involved in atherosclerosis: a systematic and bioinformatics approach. *Front Genet,* 11 (2020) 734.

12 Fonseka P, Pathan M, Chitti SV, Kang T & Mathivanan S, FunRich enables enrichment analysis of OMICs datasets. *J Mol Biol*, 433 (2021) 166747.

13 Sherman BT, Hao M, Qiu J, Jiao X, Baseler MW, Lane HC, Imamichi T & Chang W, DAVID: a web server for functional enrichment analysis and functional annotation of gene lists (2021 update). *Nucleic Acids Res,* 50 (2022) W216.

14 Cui D, Yuan W, Chen C & Han R, Identification of colorectal cancer-associated macrophage biomarkers by integrated bioinformatic analysis. *Int J Clin Exp Pathol*, 14 (2021) 1.

15 Valizadeh M, Bangash AH, Hayati D, Jafari A & Rajabi-Maham H, Assessing the Involvement of Platelet Degranulation in the Therapeutic Properties of Exosome Derived from Amniotic Epithelial Cells through Enrichment and Interaction Network Analysis. *bioRxiv*, (2021) 2021.

16 Gao Z, Jiang C, Zhang J, Jiang X, Li L, Zhao P & Li J, Hierarchical graph learning for protein–protein interaction. *Nat Commun*, 14 (2023) 1093.

17 Bader GD & Hogue CW, an automated method for finding molecular complexes in large protein interaction networks. *BMC Bioinform,* 4 (2003) 1.

18 Li CY, Cai JH, Tsai JJ & Wang CC, Identification of hub genes associated with development of head and neck squamous cell carcinoma by integrated bioinformatics analysis. *Front Oncol*, 10 (2020) 681.
19 Du L, Liu Q, Fan Z, Tang J, Zhang X, Price M, Yue B & Zhao K, Pyfastx: a robust Python package for fast random access to sequences from plain and gzipped FASTA/Q files. *Brief Bioinform,* 22 (2021) 368.
20 Patt MV, Solanki J & Georrge JJ, *In Silico* Analysis of Hypothetical Proteins of Haemophilus Influenzae PittGG Strain. *Proc Biol Sci (NCIBS)*, 14 (2020).
21 Waterhouse A, Bertoni M, Bienert S, Studer G, Tauriello G, Gumienny R, Heer FT, de Beer TA, Rempfer C, Bordoli L & Lepore R, SWISS-MODEL: homology modelling of protein structures and complexes. *Nucleic Acids Res,* 46 (2018) 296.
22 Maulana FA, Ambarsari L & Wahyudi ST, Homology modelling and structural dynamics of the glucose oxidase. *Indones J Chem*, 20 (2020) 43.
23 Hosen MI, Mia ME, Islam MN, Khatun MUS, Emon TH, Hossain MA & Miah MA, In-silico approach to characterize the structure and function of a hypothetical protein of Monkeypox virus exploring Chordopox-A20R domain-containing protein activity. *Antivir Ther*, 29 (2024) 13596535241255199.
24 Alzahrani SM, Al Doghaither HA, Al-Ghafari AB & Pushparaj PN, 5-Fluorouracil and capecitabine therapies for the treatment of colorectal cancer. *Onco Rep*, 50 (2023) 1-16.
25 Paroha S, Verma J, Dubey RD, Dewangan RP, Molugulu N, Bapat RA, Sahoo PK & Kesharwani P, Recent advances and prospects in gemcitabine drug delivery systems. *Int J Pharm*, 592 (2021) 120043.
26 Afolabi R, Chinedu S, Ajamma Y, Adam Y, Koenig R & Adebiyi E, Computational identification of *Plasmodium falciparum* RNA pseudouridylate synthase as a viable drug target, its physicochemical properties, 3D structure prediction and prediction of potential inhibitors. *Infect Genet Evol*, 97 (2022) 105194.
27 Baroroh U, Biotek M, Muscifa ZS, Destiarani W, Rohmatullah FG & Yusuf M, Molecular interaction analysis and visualization of protein-ligand docking using Biovia Discovery Studio Visualizer. *Indones J Comput Bio*, 1 (2023) 22.
28 Sharma V, Panwar P, Verma P, Rahman A, Tomar B, Saha S, Gairola N, Jakhmola V, Dangwal A & Ansori AN, Molecular docking, synthesis and in vitro alpha amylase activities of newer generation imidazolo-pyrimidine derivatives. *Adv J Chem*, (2024) 630.
29 Elsayed DA, Abdu ME, Marzouk MA, Mahmoud EM, El-Shwiniy WH, Spring AM & Shehab WS, Bio-computational modeling, POM analysis and molecular dynamic simulation for novel synthetic quinolone and benzo [d] [1, 3] oxazine candidates as antimicrobial inhibitors. *Sci Rep*, 14 (2024) 28709.
30 Azad I, Anand P, Ahmad N, Hassan F, Faiyyaz M & Akhter Y, Determination of anticancer activity and mechanism of action of benzooxazepines (BZOs) derivatives using multipronged computational and structural approaches. *Chem Phys*, 581 (2024) 112243.
31 Rahman SU, Rehman NU, Aschner M & Khan H, Antidepressant, anxiolytic sedative and muscle relaxant activities of *Nicotiana plumaginifolia* in mice. *PHYTO Nutri*, (2023) 09.
32 Chedik L, Mias-Lucquin D, Bruyere A & Fardel O, *In Silico* prediction for intestinal absorption and brain penetration of chemical pesticides in humans. *Int J Environ Res Public Health*, 7 (2017) 708.
33 Lindberg A, Chassé M, Varlow C, Pees A & Vasdev N, Strategies for designing novel positron emission tomography (PET) radiotracers to cross the blood–brain barrier. *J Label Compd Radiopharm*, 9 (2023) 2.